

Non-Linear Analog Coding for Image Transmission over Noisy Channels*

Zhi Li¹, Riley Kilfoyle², Zixiang Xiong², and Javier Garcia-Friis¹

¹Dept of Electrical and Computer Engineering, University of Delaware, Newark, DE 19716

²Dept of Electrical and Computer Engineering, Texas A&M University, College Station, TX 77843

Abstract

We propose a novel analog joint source-channel coding system for image transmission over noisy channels. First, a variable density compressive sensing encoder is applied to the desired image. Then, the resulting compressive measurements are encoded using a recently proposed non-linear analog encoder, which can operate in a rate-less fashion and produces continuous amplitude symbols that are directly transmitted over the noisy channel. Due to the non-uniform energy allocation resulting from the compressive sensing encoder, the non-linear encoder has to be carefully designed following the insights provided by an optimization analysis. Simulation results show the potential of the proposed framework, which completely skips the digital domain (bits are never utilized during the encoding process).

1 Introduction

Compressive sensing (CS) [1–5] has been one of the most important recent innovations in the field of signal processing in general, and image processing in particular. By obtaining randomized non-adaptive linear projections from the original image, which is sparse in the proper domain, CS manages to produce efficient, dimensionally reduced representations of the signal of interest at a rate lower than Nyquist’s. Reconstruction is performed by solving an inverse problem, e.g., by greedy pursuit in a basis where the original signal admits a sparse representation.

Compressive sensing can be integrated in a digital communication system in exactly the same manner as standard schemes based on sampling. In order to do so, a source encoder would first be applied to the CS measurements, producing a sequence of bits, and then these bits would be protected by applying channel coding. Provided that the source encoder and the channel encoder are optimal, and by properly fixing the rates dedicated to the source and channel encoders (for a fixed end-to-end overall information rate), the digital system will be asymptotically optimal for increasing block lengths. However, the price to pay is the need to use i) very powerful, and complex, vector quantizers to approach the rate distortion limit and ii) sophisticated channel codes such as Low-Density Parity Check (LDPC) codes that approach the channel capacity. In addition to the aforementioned complexity issues, approaching the theoretical limits requires the use of long block lengths, with the consequent delays. Moreover, digital systems

are not robust against changes in the channel conditions, since they have to be specifically designed for a desired signal to noise ratio, SNR: If the real SNR is lower than that utilized for the design, the channel encoder breaks down and the distortion will increase substantially. On the other hand, if the real SNR is higher than expected, the resulting distortion does not show any improvement.

In order to deal with the aforementioned issues, in this paper we propose to integrate compressive sensing in a discrete-time, analog-amplitude communications system that completely skips the digital domain (i.e., bits are never used in the encoding or decoding processes). The idea is to encode the measurements proceeding from the compressive sensing block utilizing very simple non-linear analog codes that directly produce the symbols to be transmitted through the channel. Different from our previous work, where non-linear transformations based on space-filling curves were used [6], we utilize a family of recently proposed non-linear codes consisting of the concatenation of soft quantization and analog linear coding. As opposed to [6], the new non-linear codes can be utilized in a rate-less manner, and are decoded utilizing message passing, which means that they can be easily adjusted to the statistics of the source/channel of interest. As we will see in the sequel, non-linear processing of the CS measurements is key, since it is well known in the literature [7] that linear coding of real numbers performs extremely poorly at high SNRs (horizontal SDR asymptote). This explains why stand-alone CS systems, where the CS measurements are directly transmitted through the noisy channel, do not achieve good performance.

2 Proposed Framework

Fig. 1 illustrates the communications framework proposed in this paper. In the first stage, variable density compressive sensing is applied to the image of interest to compress the $L \times L$ original image pixels to kM samples. The second stage is an application of a family of non-linear analog encoders to the kM compressed samples, resulting in a total number of M samples that are directly transmitted through the noisy channel. Parameter k defines the trade-off between the compressive sensing block and the analog non-linear encoder. Notice that when k is high most of the compression is performed in the analog encoder, while if k is low most of the compression is done in the compressive sensing block. As we will see in the sequel, in order to optimize performance, k must be chosen as a function of the SNR of interest and the optimal value of k will increase with the SNR. The reason is that compressive

*Work supported by NSF CCF grants 2007527 and 2007754.

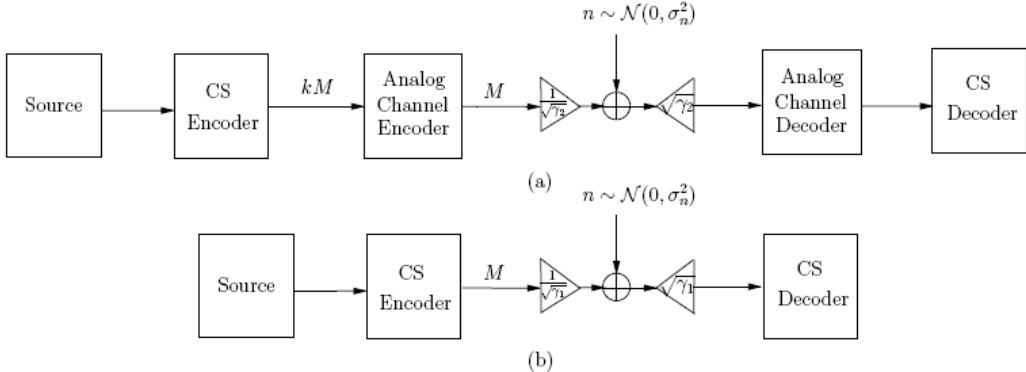


Figure 1: (a) Proposed system model: variable density compressive sensing produces kM measurements, and the number of transmitted samples is further reduced to M by applying an analog non-linear code; (b) Stand-alone CS: variable density compressive sensing produces M measurements that are directly transmitted through the channel. The number of transmitted samples in (a) and (b) is the same.

sensing is a particular case of analog linear coding, and as it is well known in the literature [7], analog linear codes perform very poorly at high SNRs (their achievable SDR is limited by an horizontal asymptote that depends on their rate).

Next, we describe in detail the system that we will use in our simulations as well as its constituent blocks (variable density compressive sensing and the novel non-linear analog codes mentioned above). We will also discuss a general analytical optimization procedure to allocate the rates and energies to the non-linear analog codes utilized in our system, which will provide insights for the design of a practical system in our simulations.

3 Variable Density CS Encoder

In this work, we adopted the variable density CS scheme of [8] because 1) it exploited the *a priori* information of the statistical distributions that natural images exhibit in the wavelet domain, 2) it reduced the necessary number of measurements for image reconstruction, and 3) it can be applied to several transform domains with simple implementation.

This section begins with an outline of the compressive sensing algorithm applied for source encoding and source decoding in the proposed JSCC scheme. It then walks through the implementation details discussing selection of transform domain, construction of the sampling matrix, and finally reconstructing the image from the transmitted data via convex optimization techniques.

3.1 CS of Natural Images

Compressive Sensing as a source coding technique for 2D images is well suited for images when applied in a transform domain wherein the image signal can be considered sparse. To be sparse in a domain, a signal $x \in \mathbb{R}^N$, must be capable of being represented by a linear combination of some subset of the basis vectors for the transform domain, $x = \Psi\theta$ where θ is an $N \times 1$ vector with zeros values for entries wherein the sparse data is non-present and Ψ is the basis $\Psi = [\psi_1, \psi_2, \dots, \psi_N]$ of the transform domain wherein x is being represented. It

has been shown in [4] that natural images are well represented via this sparse signal model when viewed in a frequency domain. For the CS source encoder, sensing is performed in the transform domain. The CS measurements are calculated by $y = \Phi\Omega x$ where Φ is a $M \times N$ matrix with $M \ll N$. With the consideration of zero-mean additive white Gaussian noise (AWGN), the measurements become $y = \Phi\Omega\theta + n$. As shown in [5], x can be recovered from y with high probability when $C\log N \ll N$, where $C \geq 1$ is an over sample factor and S is the number of linear combinations of Ψ (Sparseness) required to represent x .

3.2 CS in Ordered DHT Domain

Selection of transform domain and sampling matrix in variable density CS are directly intertwined to leverage 2-D natural image wavelet distributions.

The ordered discrete Hadamard transform (DHT) transform is suitable for analog source coding of images because it is composed of strictly binary measurement matrices and fast transform techniques are available. This is due to the basis images of the ordered DHT being binary. In an ordered DHT, the atoms are ordered according to the number of zero crossings between each entry. DHT is a transform into the generalized frequency domain, similar to a DFT. More specifically, it is most similar to the DCT of which it can be considered a binary approximation. An additional benefit of the DHT is that the result is entirely real with no imaginary components, thus simplifying calculations and matrix dimensions.

Sampling in the Hadamard domain is analogous to sampling in the DCT domain. 2-D natural images are composed of wavelets which are found in non-uniform distributions. To leverage the patterns typically found in natural images, the random selection matrix should match these patterns. The distribution pattern of the sub-band coefficients of the wavelets has been shown to be well modeled by the Generalized Gaussian Distribution (GGD) model [9]. Using the GGD as our model then the 2-D sampling probability distribution matrix can be formulated as $\rho_H(m, n) = \exp\left[-\frac{\sqrt{(\frac{m}{M})^2 + (\frac{n}{N})^2}^{\alpha_H}}{\sigma_H^2}\right]$

where $\rho_H(m, n)$ is the binary probability at index (m, n) of sampling that specific coordinate of the transformed image. $0 \leq m \leq M - 1$, $0 \leq n \leq N - 1$. The value of σ_H is used to control the total number of samples taken. Calculation of σ_H is performed through numerical method by a binary search tree algorithm to sample the desired number of points. An example $\rho_H(m, n)$ for selection of $k = 15,000$ points (out of 65536 total) is shown in Fig. 2. The 2-D exponential decay pattern of the sample energy as predicted by a GGD is seen in Fig. 3.

Values from 1-5 for α were simulated in [8] and α_H is arbitrarily set to 2.65 for our calculations as this was demonstrated empirically to perform well across a variety of images in previous research [10].

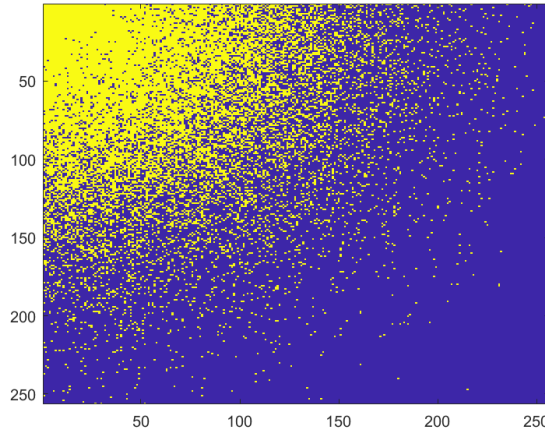


Figure 2: CS Random Sampling Matrix for 15,000 Samples.

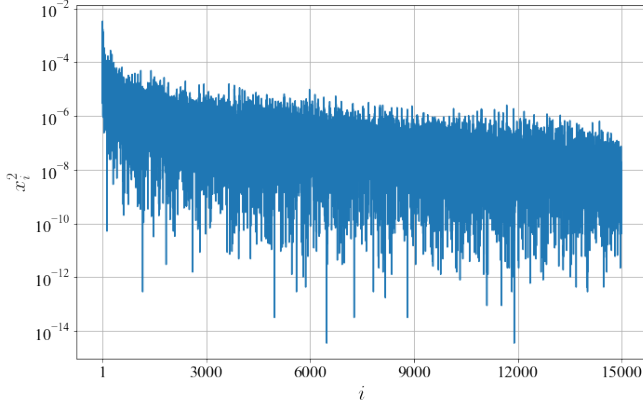


Figure 3: Energy per sample for the 15,000 CS measurements of the image ‘boat’. Notice that the energy decreases with the measurement number.

3.3 Reconstruction of Sampled Images

Reconstruction of the original signal can be performed via an iterative convex optimization solver minimizing the two following terms. Variation, $V(y) = \sum |y_{n+1} - y_n|$ and Mean Squared Error (MSE), $E(x, y) = \frac{1}{n} \sum (x_n - y_n)^2$. Total Variation (TV) to be minimized is then $E(y, \bar{x}) + \lambda V(\bar{x})$ where the value λ is a control parameter weighting the importance of

MSE against variation in the reconstruction. The constraint on the minimization is an inequality constraint that $y - \Phi_\Omega \bar{x} \leq \epsilon$ where \bar{x} is the reconstruction of original signal x , y is the noisy measurement vector described previously, and ϵ is the upper bound on the difference between the transform of the reconstructed \bar{x} and the received vector y . In order to aid solver convergence, the initial \bar{x} starting point for the solver is specified as the back projection of the received vector, $\Phi_\Omega^{-1}y$.

4 Non-Linear Analog Coding

In this section we first provide an overview of the non-linear analog codes proposed by some of us in [11], where the input symbols were realizations of an Independent and Identically Distributed (iid) Gaussian random variable of mean 0 and variance 1. Then we explain how to use this family of analog codes to encode the kM compressive sensing samples obtained as explained in the previous CS section.

4.1 Analog Coding for iid Gaussian input symbols

The non-linear analog codes proposed in [11] produce the output symbols by linearly encoding sample-by-sample shifted versions of the input samples. Those output symbols will then be sent directly through the noisy channel. Thus, the encoder proceeds in two steps. First, the standard scalar quantizer characteristic of digital communication systems is replaced by a sample-by-sample shifting transformation (non-linearity), outputting an intermediate vector of real numbers. As in a standard quantizer, the input space is partitioned into regions, but instead of assigning a different centroid to each region, all the input source samples in the same region are shifted by the same specific value, which varies across different regions. In this way, after shifting the regions are separated from each other, and the shifting process can be seen as a soft quantizer. In the second step, the output symbols are obtained by linearly transforming the aforementioned intermediate vector of shifted samples. They are then normalized to the desired average energy per symbol, E_s , and directly transmitted through an Additive White Gaussian Noise (AWGN) channel of mean zero and variance σ_n^2 . Finally, the decoder obtains the estimated vector of input samples by processing the received noisy sequence.

As explained in [11], in order to obtain good performance for a specific SNR, it is key to optimize the number of regions, Q , and the shifting values that are applied to each one of the regions. Indeed, as we discussed above the discontinuities introduced by the shifting step can be seen as an extension of what a standard quantizer does¹. For simplicity, we will partition the input space into regions that are optimal for the scalar quantization of a Gaussian random variable [12], which is sub-optimal in our joint source-channel coding framework but simplifies the design procedure. Fig. 4 shows the distribution of

¹Notice that discontinuities always appear in analog codes, such as in space-filling curves, existing in the literature: linear analog codes have very poor performance, and the discontinuities act as the non-linearities required for good performance.

the intermediate vector of shifting samples when $Q = 4$ (recall that the input is Gaussian.) Since the interval length of a region is fixed, the shifting transformation, S' , which must be symmetric with respect to the y-axis as the input distribution (Gaussian) and the regions also present that symmetry, is perfectly defined by providing the separation between the transformed regions in $\mathbb{R}+$, $\{l_0, l_1, l_2 \dots\}$ when Q is odd. For even Q , l_0 specifies the separation between the transformed regions in $\mathbb{R}+$ and $\mathbb{R}-$ which are closest to 0 and $\{l_1, l_2 \dots\}$ are the separations between the transformed regions in $\mathbb{R}+$. The final shifting transformation, S , is constructed by normalizing S' , so that the variance of the prior for the intermediate shifted nodes is the same as that of the source nodes (unit variance in this subsection).

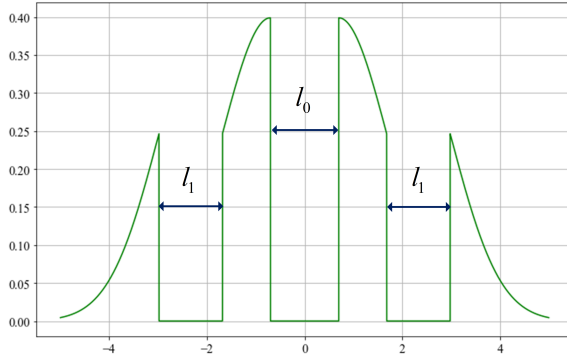


Figure 4: Probability density function of the prior for the intermediate shifted samples when $Q = 4$.

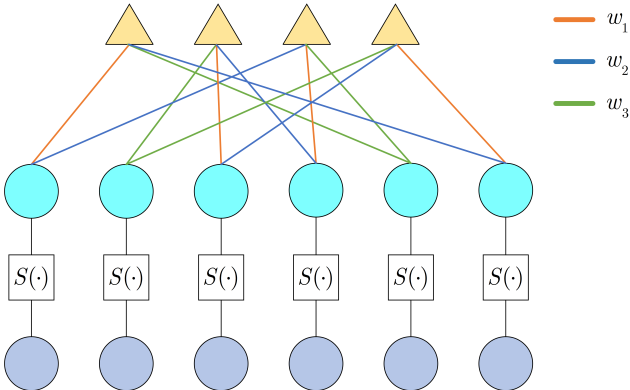


Figure 5: Proposed scheme that encodes six Gaussian samples into four output symbols. Each symbol is generated by the linear combination of a subset of the source samples shifted by the function S .

As shown in Fig. 5, the linear encoding performed in the second step of the encoding process can be represented as a weighted graph, where each output (transmitted) symbol is generated as a weighted linear combination of a random subset of d_r “shifted” nodes proceeding from the first step. The value of d_r should be small to generate a sparse graph in which decoding can be performed using message passing [13]. Different from typical message passing utilized in digital communication systems, here we deal with continuous random variables. Thus, the messages that are exchanged in the decod-

ing process are the probability density functions of the random variables of interest. The objective is to obtain the estimates of the source symbols that minimize the mean squared error. This is achieved by estimating the posterior probability density function of the intermediate vector of shifted samples in an iterative manner. Then, the posterior probability density function of each one of the source samples is obtained through the inverse shifting transformation, and the estimate of each one of the source samples is calculated as the mean of the corresponding posterior probability density function. The detailed equations can be seen in [11], where the proposed system is shown to achieve an excellent performance for the transmission of Gaussian sources over AWGN channels.

4.2 Analog coding of the CS measurements: Theoretical analysis

Fig. 3 shows the energy per sample of the CS measurements when $kM = 15,000$. Notice that the energy decreases along the x-axis. This means that the proposed non-linear analog codes described in the previous subsection have to be adapted to this situation in which the input samples are not identically distributed. As a first approximation, we will model the kM CS measurements as the concatenation of P bands, with each band $i = 1 \dots P$ consisting of K_i iid Gaussian samples of mean 0 and variance σ_i^2 . In the more general case, depicted in Fig. 6, which we will consider for the analysis in this subsection, each band can be encoded with a different analog code, so that the N_i encoded samples of band i , each one of them with energy per sample E_i , will be directly transmitted through an AWGN channel of mean zero and variance σ^2 . Notice that $\sum_i K_i = kM$ and $\sum_i N_i = M$ so that the overall information rate for the analog encoder is k . Decoding will be performed independently for each band.

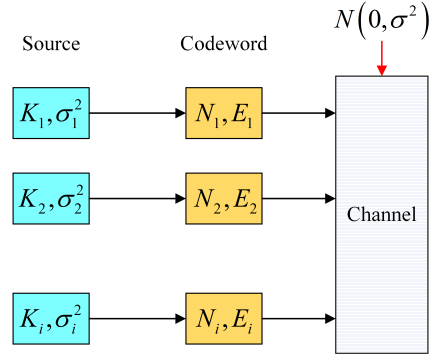


Figure 6: Framework for the proposed multi-band analysis.

The theoretical limit for the aforementioned multi-band transmission scheme can be obtained by minimizing the distortion per sample of the decoded vector. Since each band is modeled as a Gaussian source generating iid samples of mean zero and variance σ_i^2 , the minimum distortion per sample for each band is obtained equaling $K_i R(D_i) = N_i C$, where $R(D_i)$ is the rate distortion of the band and C is the channel capacity. We then obtain

$$\begin{aligned} \frac{K_i}{2} \log \frac{\sigma_i^2}{D_i} &= \frac{N_i}{2} \log \left(1 + \frac{E_i}{\sigma^2}\right) \\ \Rightarrow D_i &= \frac{\sigma_i^2}{\left(1 + \frac{E_i}{\sigma^2}\right)^{N_i/K_i}}. \end{aligned} \quad (1)$$

The optimization problem is formulated as

$$\begin{aligned} \min_{N_i, E_i} \quad & \frac{\sum_i K_i D_i}{m} \\ \text{s.t.} \quad & \sum_i N_i = n \\ & \frac{\sum_i N_i E_i}{n \sigma^2} = 10^{\text{SNR}/10} \\ & N_i \geq 0, E_i \geq 0, \end{aligned} \quad (2)$$

where SNR is the desired signal to noise ratio in dB (different SNRs will lead to different results in the optimization problem). By defining the constants B_1 and B_2 as $B_1 = n$ and $B_2 = 10^{\text{SNR}/10} * n \sigma^2$ and assuming $K_i = K$ for all i , the objective function reduces to minimizing $\sum_i D_i$. According to the Kuhn-Tucker conditions, the optimization problem is equivalent to solving

$$\begin{aligned} F(N_i, E_i, \alpha, \beta, \lambda_i, \gamma_i) &= \sum_i \frac{\sigma_i^2}{\left(1 + \frac{E_i}{\sigma^2}\right)^{N_i/K}} \\ + \alpha(\sum_i N_i - B_1) + \beta(\sum_i N_i E_i - B_2) + \lambda_i N_i + \gamma_i E_i \\ \frac{\partial F}{\partial N_i} = 0, \frac{\partial F}{\partial E_i} = 0, \frac{\partial F}{\partial \alpha} = 0, \frac{\partial F}{\partial \beta} = 0, \\ \lambda_i N_i = 0, \lambda_i \geq 0, N_i \geq 0, \gamma_i E_i = 0, \gamma_i \geq 0, E_i \geq 0. \end{aligned} \quad (3)$$

Taking the partial derivative with respect to N_i and E_i , we obtain

$$\begin{aligned} \frac{\partial F}{\partial N_i} &= -\frac{\sigma_i^2 (1 + \frac{E_i}{\sigma^2})^{-N_i/K}}{K} \ln \left(1 + \frac{E_i}{\sigma^2}\right) \\ &+ \alpha + \beta E_i + \lambda_i \end{aligned} \quad (4)$$

$$\frac{\partial F}{\partial E_i} = -\frac{\sigma_i^2 N_i (1 + \frac{E_i}{\sigma^2})^{-N_i/K}}{K(\sigma^2 + E_i)} + \beta N_i + \gamma_i. \quad (5)$$

Since $N_i \geq 0$ and $E_i \geq 0$, it means $\lambda_i = 0$, $\gamma_i = 0$ (otherwise $N_i = E_i = 0$). Solving for λ_i and γ_i in (4) and (5) and setting them equal to 0, we arrive at

$$\beta(\sigma^2 + E_i) \ln \left(1 + \frac{E_i}{\sigma^2}\right) = \alpha + \beta E_i, \quad (6)$$

where α and β are constants which are independent of i . Notice that (6) shows that E_i is also independent of i , and, therefore, the optimal E_i is equal to B_2/B_1 for all i . Therefore, the multivariate optimization problem (3) is reduced to P univariate optimization problems consisting of solving for N_i in (4)

when $\beta = 0$, which results in

$$\begin{aligned} N_i &= \max \left\{ 0, -\frac{K}{\ln t} \ln \frac{\alpha K}{\sigma_i^2 \ln t} \right\}, \\ \text{where } t &= 1 + \frac{E}{\sigma^2}. \end{aligned} \quad (7)$$

The Lagrange multiplier α can be obtained by using the constraint $\sum_i N_i = B_1$. Notice that for every desired SNR, the optimization process provides the solution, $N_i^*, i = 1 \dots P$, which can be used to calculate the corresponding SDR. Repeating the process for multiple values of SNR, we can depict the theoretical limit, in terms of SDR vs SNR, for the transmission of the compressive sensing measurements, modeled as the sequence of bands defined before, over a Gaussian channel.

Fig. 7 presents the results obtained with the optimization above for $kM = 15,000$ CS measurements of the image ‘Boat’. Specifically, we partition the vector of CS measurements in $P = 10, 15, 30, 60$ bands when the end-to-end coding rate is fixed to $R_c = k = 3$. The figure depicts three types of curves: i) SDR achieved when E_i is the same for all bands and N_i is optimized (recall E_i equal for all samples provides the best results), ii) SDR achieved when N_i is the same for all bands and E_i is optimized, and iii) SDR when the whole vector is treated as iid samples with variance equal to the average variance for the whole vector of CS measurements. It is worth noticing that for the number of bands, P , considered in Fig. 7, the results are practically independent of P . Optimizing E_i while fixing N_i results in some improvement over the case iii), but the real improvement is obtained when N_i is optimized. This is an important observation which will guide the design of our practical system in the following subsection. It is important to remark that the optimal values of N_i decrease for the bands associated to the CS measurements where the energy per sample decreases (see Fig. 3), and the difference between the maximum and minimum values of the optimal N_i 's increases as the SNR decreases.

Fig. 8 presents the results obtained with the proposed optimization method when $kM = 10,000$ CS measurements of the image ‘Boat’ are considered, the end-to-end rate is fixed to $R_c = k = 2$, and the vector of CS measurements is partitioned in $P = 10, 20, 40$ bands. The results are very similar to the ones obtained for $kM = 15,000$ CS measurements in the previous figure, but it is interesting that, independently of the SNR value, the difference between the maximum and minimum values of the optimal N_i 's is now less than in the case of $kM = 15,000$ CS measurements. This will guide our practical designs presented in the next subsection.

4.3 Analog coding of the CS measurements: Practical approach

Although, as described in the previous subsection, the optimal approach is to encode each one of the bands in an independent manner performing the proper energy (E_i) and rate (N_i) allocation among all the bands, implementing this scheme is quite involved from a practical perspective. The reason is that it requires a large number of different analog codes (as many

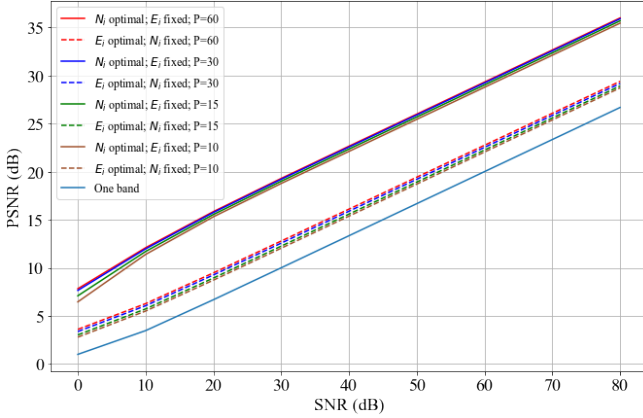


Figure 7: For $kM = 15,000$ CS measurements of the image ‘Boat’, and different number of bands, P , i) SDR achieved when E_i is the same for all bands and N_i is optimized, ii) SDR achieved when N_i is the same for all bands and E_i is optimized, and iii) SDR when the whole vector is treated as iid samples with variance equal to the average variance of the CS measurements.

as bands, P), and each has to be optimized for the desired rate. To simplify the design, we utilize a much more limited number of codes, while trying to follow the intuition gained from the optimization method described in the previous subsection, namely i) use rates close to 1 for the CS measurements with high energy per sample, ii) use rates close to 0 for the CS measurements with very low energy per sample, iii) use codes of intermediate rates (between 0 and 1) for CS measurements with intermediate energy per sample. In the proposed implementation, we use a simplified version of these guidelines as follows:

- We start with kM CS measurements.
- The first L_I CS measurements are transmitted directly through the channel, each with energy proportional to its amplitude (same proportionality factor, γ , for all the L_I measurements.)
- The last L_E CS measurements are not transmitted.
- The remaining $L = kM - L_I - L_E$ measurements are transmitted using one of the non-linear analog codes described in the previous section, which will have a rate close to k so that the total number of channel uses is M .

The parameters to optimize in our practical implementation are k , L_I , γ , L_E , and the parameters of the non-linear code: number of regions Q and separation among regions $\{l_0, l_1, \dots\}$ for the shifting stage, which may be different for nodes coming from different bands, and d_r . The decoding of the non-linear analog code is done in exactly the same manner as in the previous subsection, except that for a specific input node the prior depends on the band to which it belongs (recall that each of the P bands has a different variance). To facilitate the encoding/decoding process, the L input symbols are permuted and

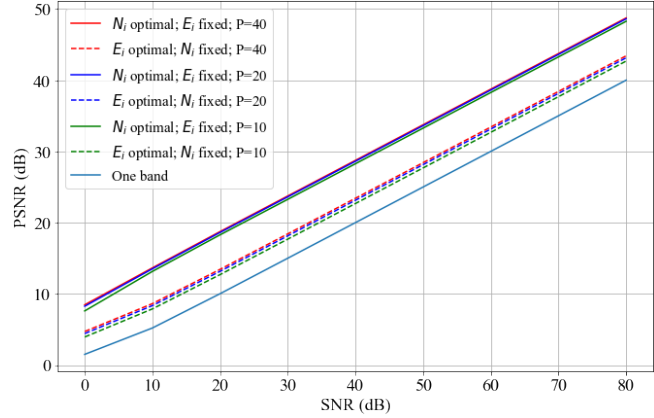


Figure 8: For $kM = 10,000$ CS measurements of the image ‘Boat’ and different number if bands P , i) SDR achieved when E_i is the same for all bands and N_i is optimized, ii) SDR achieved when N_i is the same for all bands and E_i is optimized, and iii) SDR when the whole vector is treated as iid samples with variance equal to the average variance of the CS measurements.

partitioned into several pieces so that all pieces are encoded independently using the same code.

5 Simulation Results

In order to assess the performance of the proposed framework, we apply it to the 256×256 image ‘Boat’. As discussed previously, we first perform CS to obtain kM measurements, and then we apply the proposed non-linear codes so that we always transmit M symbols through the noisy channel. We fix $M = 5,000$ and, in addition to the trivial case of $k = 1$, we consider $k = 2$ and $k = 3$. For each one of these cases, we perform Monte Carlo simulations to ‘optimize’ for parameters $L_I, \gamma, L_E, Q, \{l_0, l_1, \dots\}$ and d_r .

The results in terms of SDR vs SNR for the best systems at each SNR are presented in Fig. 9, while Tab. 1 and Tab. 2 show the parameters of the utilized systems. As expected, at high SNR the systems based on $k = 3$, which is the value of k for which the non-linear code performs the highest amount of compression, perform best, while the stand-alone system ($k = 1$) is the best for low SNR. The reason is that linear codes, of which compressive sensing is an example, behave poorly at high SNRs, since they achieve an asymptotic distortion which does not diminish when the SNR increases. Therefore, the minimum distortion achieved by the proposed scheme at high SNR values will be determined by the compressive sensing block, and will decrease when k increases.

Fig. 10 shows the reconstructed images and their corresponding PSNRs when SNR=80 dB. As expected, the best performance at high SNR is obtained when $k = 3$ and the worst occurs for $k = 1$ (standard stand-alone CS).

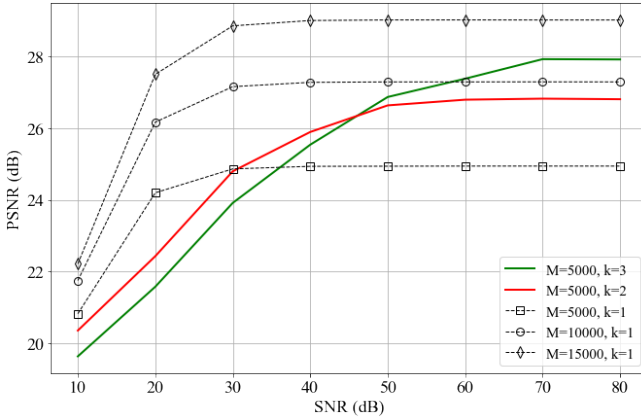


Figure 9: For the 256×256 image ‘‘Boat’’, PSNR of the reconstructed image as a function of the channel SNR when $M = 5,000$ samples are transmitted through an AWGN channel and different design parameters are used. For high SNRs, the systems with $k = 3$ outperform the ones with $k = 1$ and $k = 2$, while for medium SNRs parameter $k = 2$ leads to the best performance. The performance of the stand-alone CS system ($k = 1$) with $M = 5,000$, $M = 10,000$ and $M = 15,000$ measurements is also depicted for comparison purposes.

Table 1: Parameters of the $k = 2$ systems utilized in Fig. 9 for different SNR values.

SNR (dB)	L_I	γ	L_E	Q	l_0, l_1, l_2	d_r
10	30	0.06	30	4	10, 10, -	4
20	400	0.06	400	4	18, 2, -	4
30	400	0.06	400	4	10, 13, -	4
40	30	0.06	30	5	13, 10, -	4
50	30	0.06	30	7	10, 10, 10	4
60	30	0.06	30	7	10, 10, 10	4
70	30	0.06	30	7	10, 10, 10	4
80	30	0.06	30	7	10, 10, 10	4

6 Conclusions

We have proposed an analog joint source-channel coding system for image transmission over noisy channels consisting of two stages: A variable density compressive sensing encoder applied to the image of interest followed by non-linear analog coding applied on the CS measurements. We have used the insights gained from a theoretical analysis of the optimal energy and rate allocation to design practical codes that present excellent performance.

References

- [1] R. Baraniuk, ‘‘Compressive sensing,’’ *IEEE Signal Processing Magazine*, vol. 24, no. 4, pp.118-121, July 2007.
- [2] E. Candes, J. Romberg, and T. Tao, ‘‘Robust uncertainty principles: exact signal reconstruction from highly incomplete frequency information,’’ *IEEE Trans. on Information Theory*, vol. 52, no. 2, pp. 489-509, February 2006.
- [3] E. Candes, J. Romberg, and T. Tao, ‘‘Stable signal recovery from incomplete and inaccurate measurements,’’ *Communications on Pure and Applied Mathematics*, vol. 59, no. 8, pp. 1207-1223, August 2006.
- [4] E. Candes and T. Tao, ‘‘Near optimal signal recovery from random projections: universal encoding strategies?’’, *IEEE Trans. on Information Theory*, vol. 52, no. 12, pp. 5406-5425, December 2006.
- [5] D. Donoho, ‘‘Compressed sensing,’’ *IEEE Trans. on Information Theory*, vol. 52, no. 4, pp. 1289-1306, April 2006.
- [6] Y. Hu, Z. Wang, J. Garcia-Frias, and G. R. Arce, ‘‘Non-Linear Coding for Improved Performance in Compressive Sensing,’’ *CISS’09*, Baltimore, MD, March 2009.
- [7] K.-H. Lee and D. P. Petersen, ‘‘Optimal linear coding for vector channels,’’ *IEEE Trans. on Communications*, vol. 24, no. 12, pp. 1283-1290, December 1976.
- [8] Z. Wang and G. R. Arce, ‘‘Variable density compressed image sampling,’’ *IEEE Transactions on Image Processing*, vol. 19, no. 1, pp. 264-270, January 2010.
- [9] S. Chang, B. Yu, and M. Vetterli, ‘‘Adaptive wavelet thresholding for image denoising and compression,’’ *IEEE Trans. Image Processing*, vol. 9, no. 9, pp. 1532-1546, Sept. 2000.
- [10] J. Romberg, H. Choi and R. Baraniuk, ‘‘Bayesian tree-structured image modeling using wavelet-domain hidden Markov models,’’ *IEEE Trans. Image Processing*, vol. 10, no. 7, pp. 1056-1068, July 2001.
- [11] M. Burich and J. Garcia-Frias, ‘‘A simple family of non-linear analog codes,’’ *Submitted to IEEE Communications Letters*, June 2023.
- [12] J. Max, ‘‘Quantizing for minimum distortion,’’ *IRE Transactions on Information Theory*, vol. 6, no. 1, pp. 7-12, March 1960.
- [13] J. Pearl, ‘‘Probabilistic Reasoning in Intelligent Systems: Networks of Plausible Inference,’’ San Francisco, CA, USA: Morgan Kaufmann Publishers Inc., 1988.

Table 2: Parameters of the $k = 3$ systems utilized in Fig. 9 for different SNR values.

SNR (dB)	L_I	γ	L_E	Q	l_0, l_1, l_2	d_r
10	600	0.06	1200	5	80, 8, -	6
20	600	0.06	1200	5	80, 8, -	6
30	600	0.06	1200	4	4, 100, -	6
40	600	0.06	1200	4	120, 40, -	6
50	600	0.06	1200	5	80, 8, -	6
60	600	0.06	1200	5	80, 8, -	6
70	600	0.06	1200	7	140, 50, 10	6
80	600	0.06	1200	7	140, 50, 10	6



(a) Original 256×256 Boat image



(b) $k = 1$, PSNR=24.94 dB



(c) $k = 2$, PSNR=26.81 dB



(d) $k = 3$, PSNR=27.92 dB

Figure 10: For the original 256×256 image “Boat” represented in (a), reconstructed images corresponding to (b) $k = 1$ (stand-alone CS); (c) $k = 2$; and (d) $k = 3$ when $M = 5,000$ samples are transmitted through an AWGN channel and SNR=80 dB.